Supplementary Figure 1

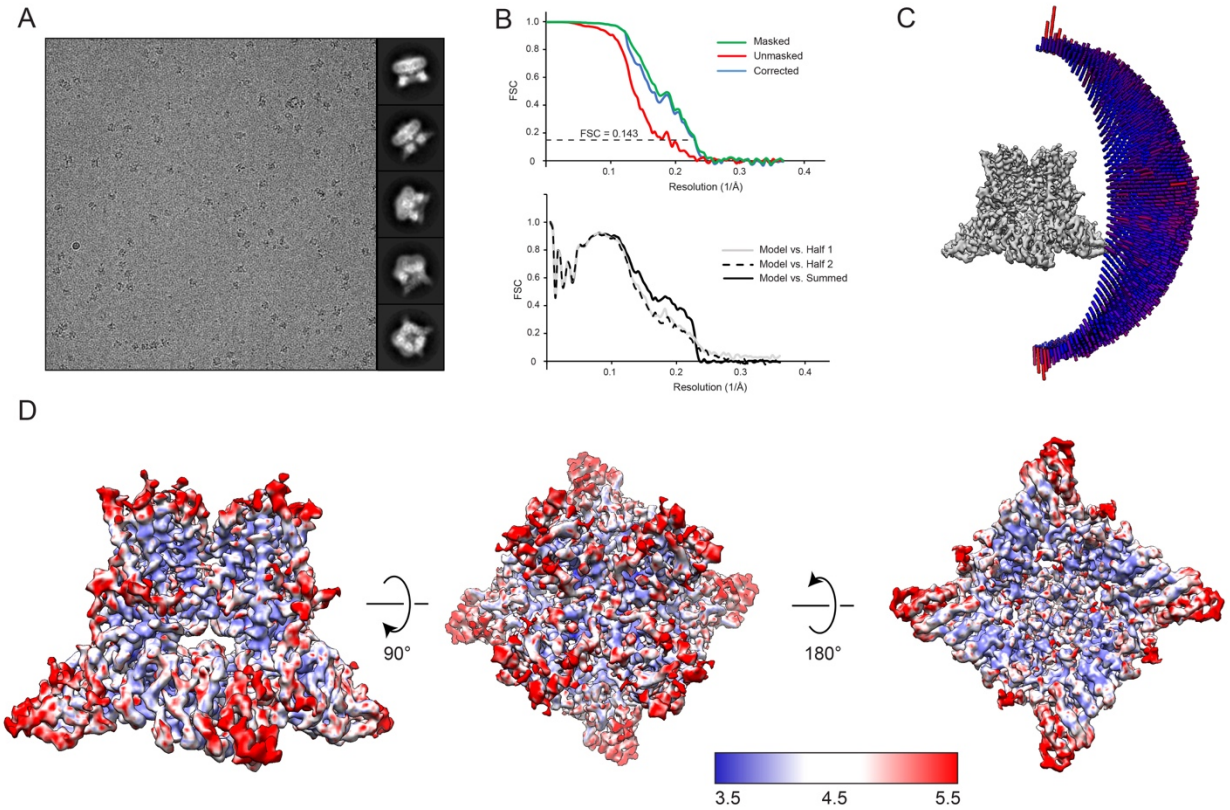

Supplementary Figure 1. EM summary of CBD-bound TRPV2 in detergent. (**A**) Representative micrograph and 2D classes of cryo-EM data. (**B**) Map FSC curves and model validation curves. (**C**) Angular distribution for final 3D reconstruction. Tall red cylinders indicate a large number of particles aligned at a position and short blue cylinders indicate fewer particles. (**D**) Top, bottom and side view of CBD-bound TRPV2 in detergent colored based on local resolution as calculated via RESMAP. Blue, white and red regions indicate resolutions of 3.5Å, 4.5Å and 5.5Å, respectively.

Supplementary Figure 2

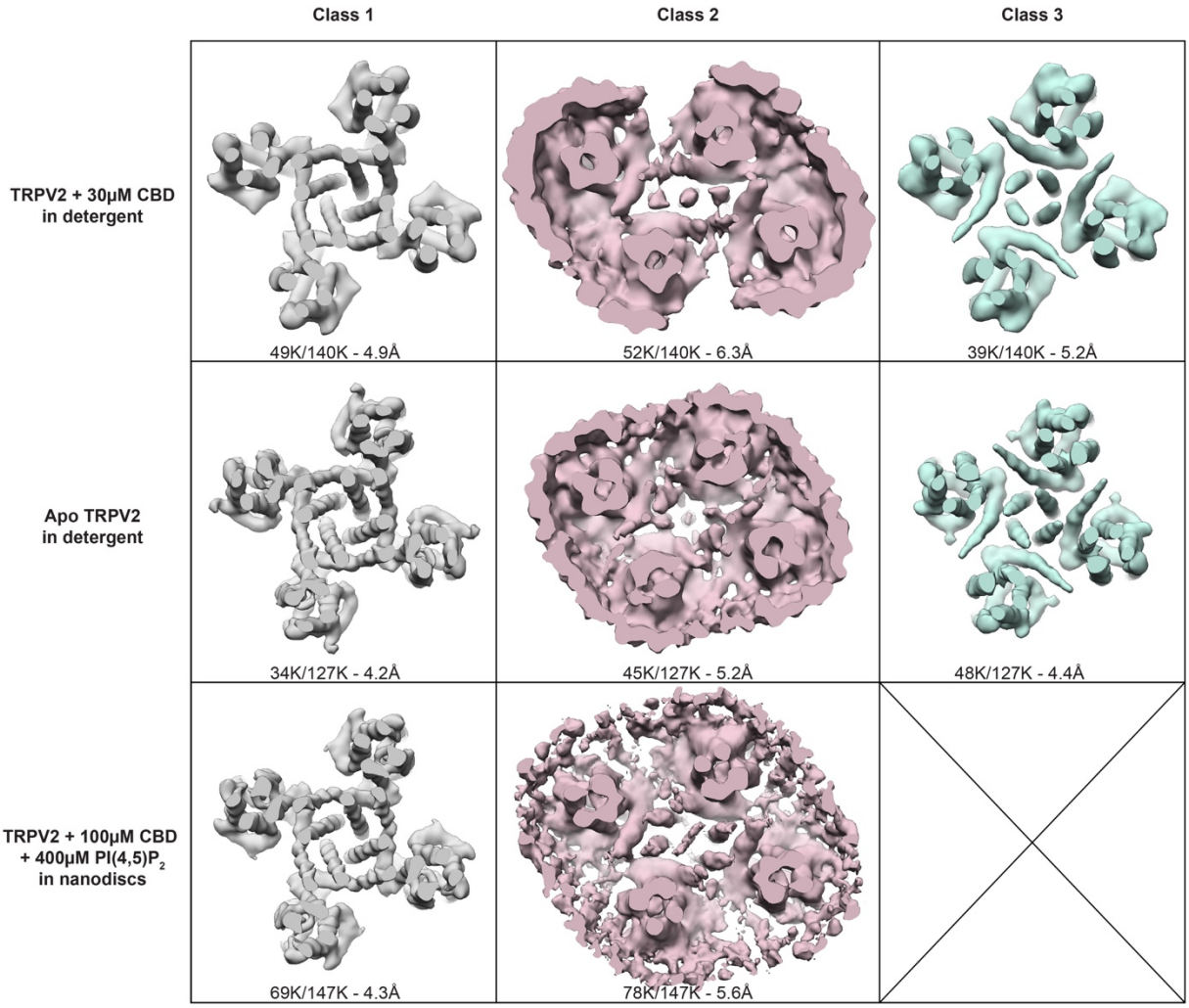

Supplementary Figure 2. Conformational flexibility of TRPV2. Slices of the EM density maps from classes seen during initial 3D classification in several purification conditions highlighting the differences in the trajectories of the helices that constitute the pore. Under each slice the number of particles for each class and the number of good particles from each dataset are listed along with the resolution of the cryo-EM density map after 3D refine. Class 1 (grey) is C4 symmetric and seen in all conditions. Class 2 (pink) is C2 symmetric and seen in all conditions. Class 3 (green) is C4 symmetric and seen only in detergent purification conditions. An 'X' through the box indicates that this state was not seen during classification.

Supplementary Figure 3

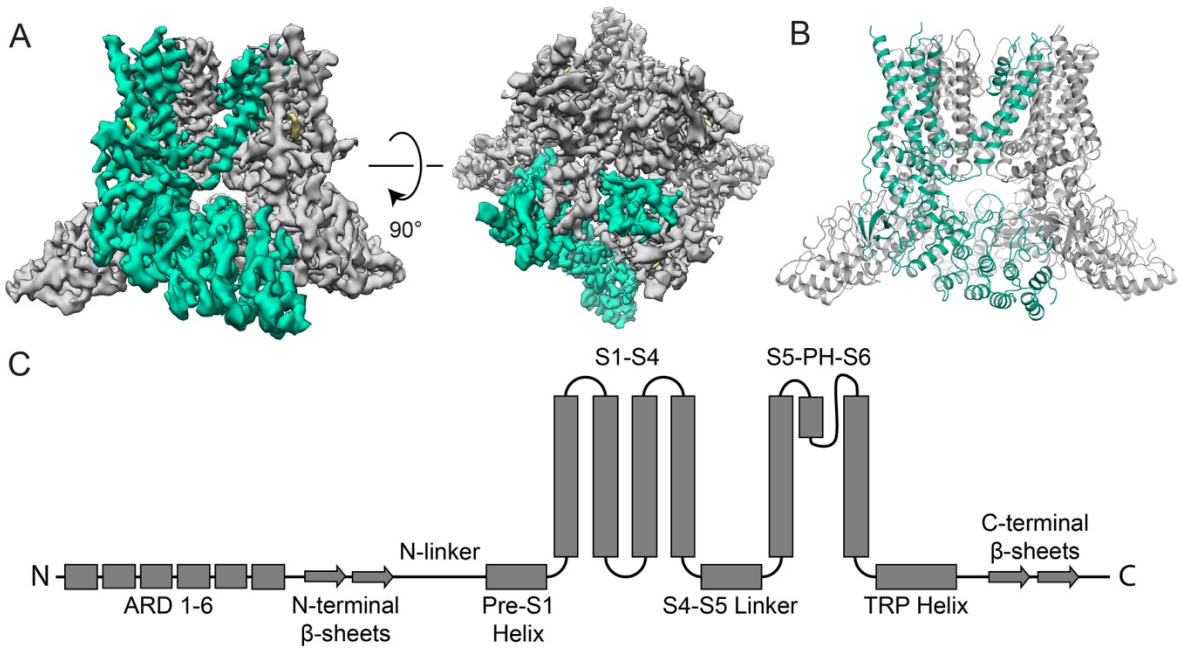

Supplementary Figure 3. CBD-bound TRPV2 in detergent. (**A**) Side and top views of the structure of CBD-bound TRPV2 in detergent solved to 4.3Å. A single monomer is colored in green and the others are shown in grey. The densities attributed to lipids are shown in khaki. (**B**) Atomic model of CBD-bound TRPV2 in detergent. A single monomer is colored in green and the others are shown in grey. (**C**) Schematic overview of TRPV2 domains.

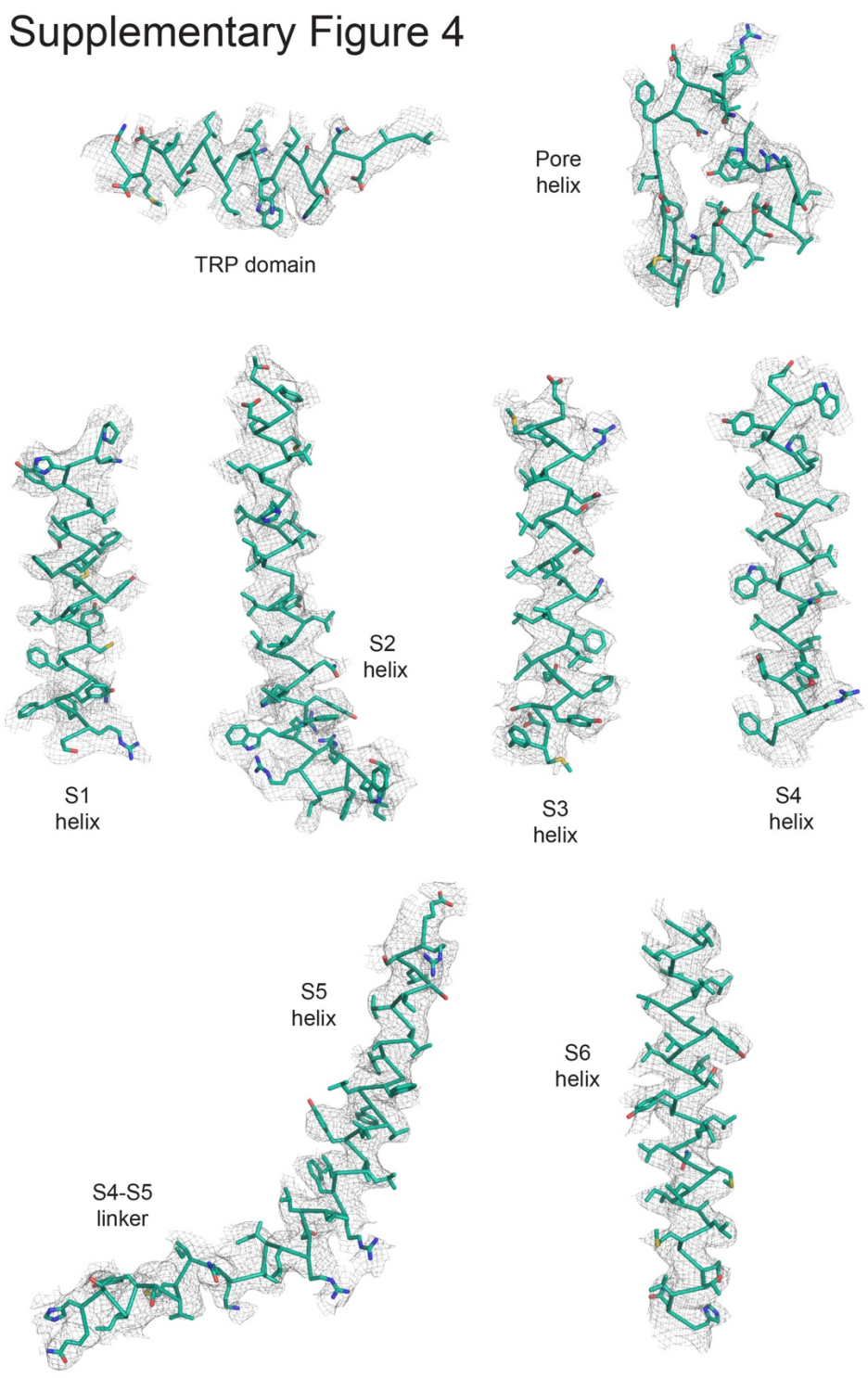

Supplementary Figure 4. Data quality of the CBD-bound TRPV2 in detergent structure. Selected helices of the CBD-bound TRPV2 in detergent model (green) overlaid with the corresponding cryo-EM density map in grey mesh. Side chains are shown as sticks and atoms are colored by element.

Supplementary Figure 5

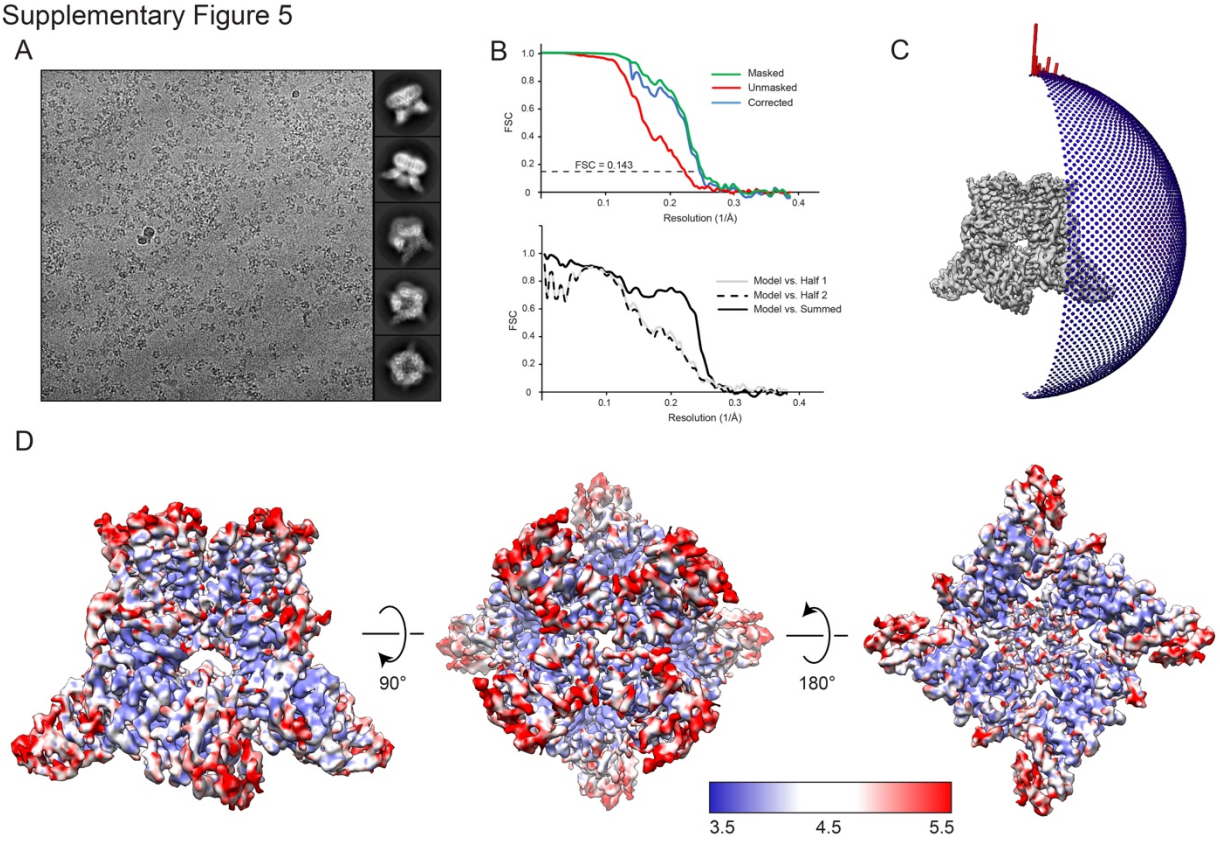

Supplementary Figure 5. EM summary of apo TRPV2 in detergent. (**A**) Representative micrograph and 2D classes of cryo-EM data. (**B**) Map FSC curves and model validation curves. (**C**) Angular distribution for final 3D reconstruction. Tall red cylinders indicate a large number of particles aligned at a position and short blue cylinders indicate fewer particles. (**D**) Top, bottom and side view of apo TRPV2 colored based on local resolution as calculated via RESMAP. Blue, white and red regions indicate resolutions of 3.5Å, 4.5Å and 5.5Å, respectively.

Supplementary Figure 6

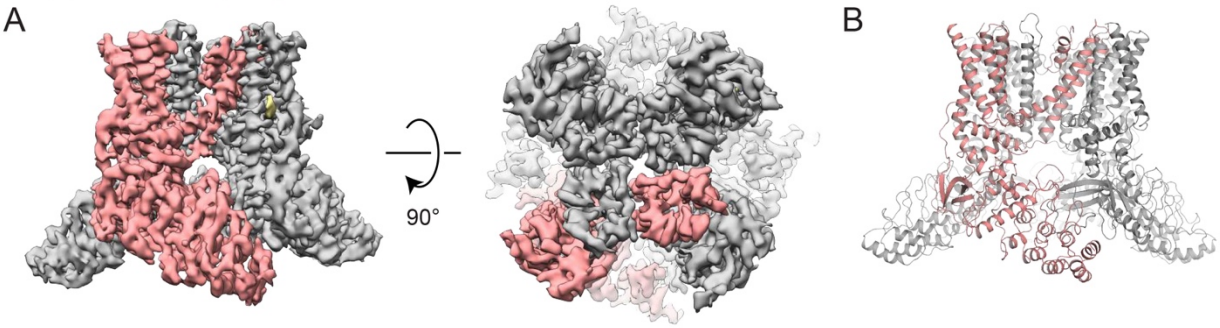

Supplementary Figure 6. Apo TRPV2 in detergent. (**A**) Side and top views of the structure of apo TRPV2 in detergent solved to 4.1Å. A single monomer is colored in salmon and the others are shown in grey. The densities attributed to lipids are shown in khaki. (**B**) Atomic model of apo TRPV2 in detergent. A single monomer is colored in salmon and the others are shown in grey.

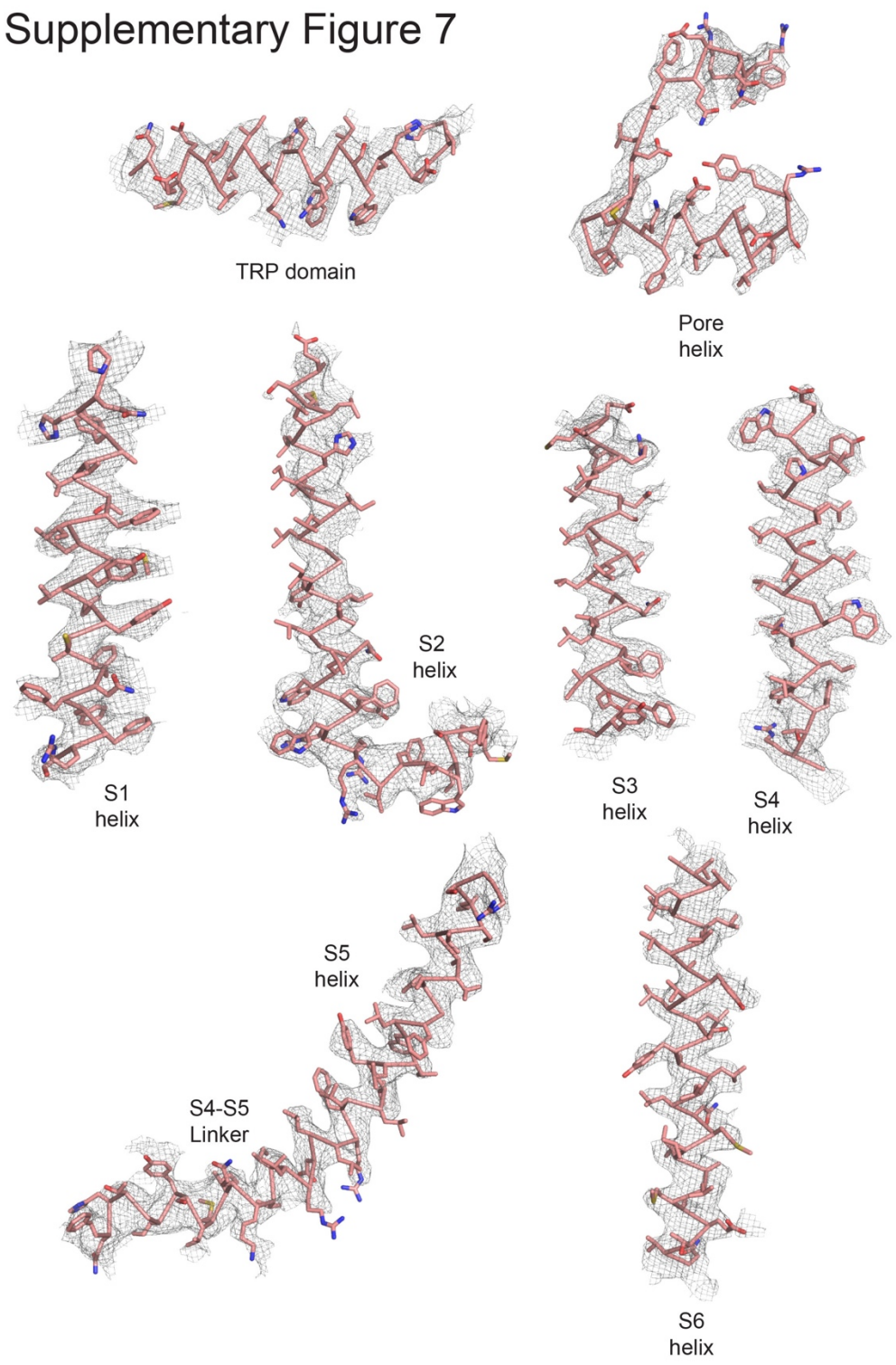

Supplementary Figure 7. Data quality of the apo TRPV2 in detergent structure. Selected helices of the apo TRPV2 model (salmon) overlaid with the corresponding cryo-EM density map in grey mesh. Side chains are shown as sticks and atoms are colored by element.

Supplementary Figure 8

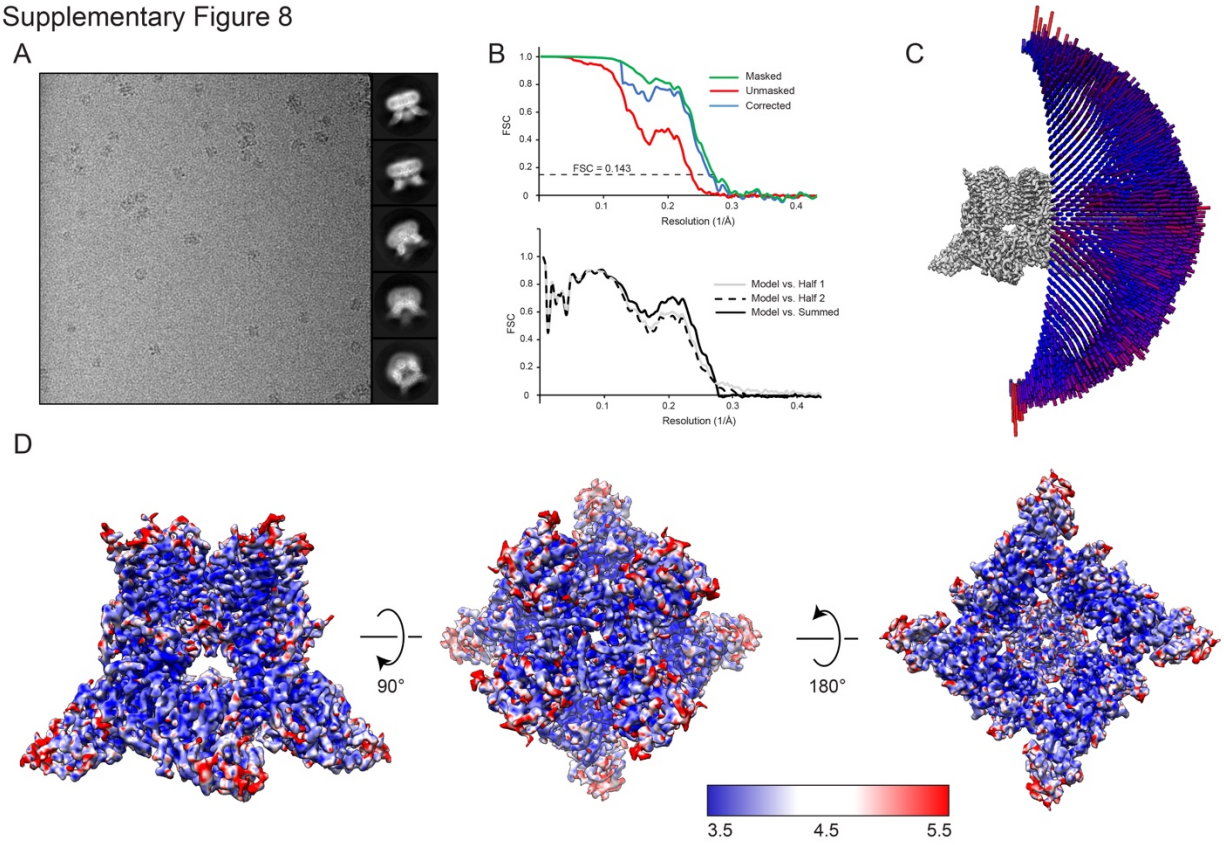

Supplementary Figure 8. EM summary of CBD-bound TRPV2 in PI(4,5)P_2 enriched nanodiscs. (**A**) Representative micrograph and 2D classes of cryo-EM data. (**B**) Map FSC curves and model validation curves. (**C**) Angular distribution for final 3D reconstruction. Tall red cylinders indicate a large number of particles aligned at a position and short blue cylinders indicate fewer particles. (**D**) Top, bottom and side view of nanodisc reconstituted CBD-bound TRPV2 in the presence of PI(4,5)P_2 colored based on local resolution as calculated via RESMAP. Blue, white and red regions indicate resolutions of 3.5Å, 4.5Å and 5.5Å, respectively.

Supplementary Figure 9

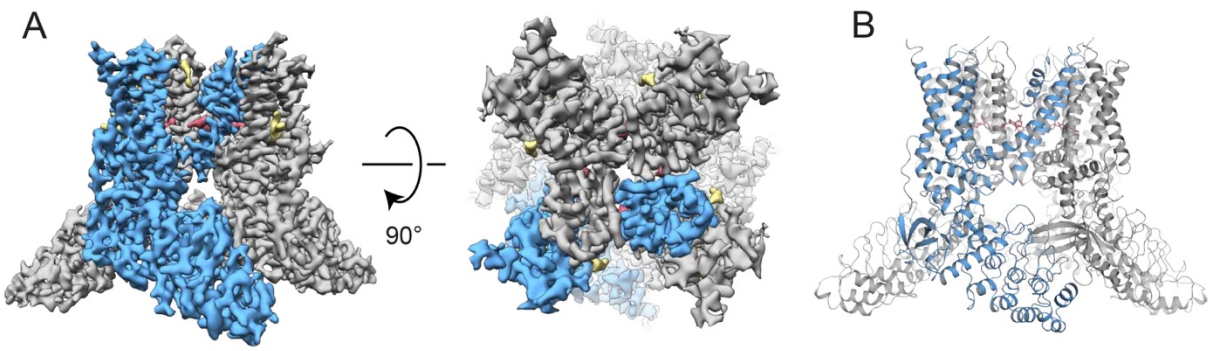

Supplementary Figure 9. CBD-bound TRPV2 in PI(4,5)P_2 enriched nanodiscs. (**A**) Side and top views of the structure of CBD-bound TRPV2 in PI(4,5)P_2 enriched nanodiscs solved to 4.1Å. A single monomer is colored in blue and the others are shown in grey. The densities attributed to bound CBD and lipids are shown in pink and khaki, respectively. (**B**) Atomic model of CBD-bound TRPV2 in PI(4,5)P_2 enriched nanodiscs. A single monomer is colored in blue and the others are shown in grey. Bound CBD is shown as pink sticks.

Supplementary Figure 10

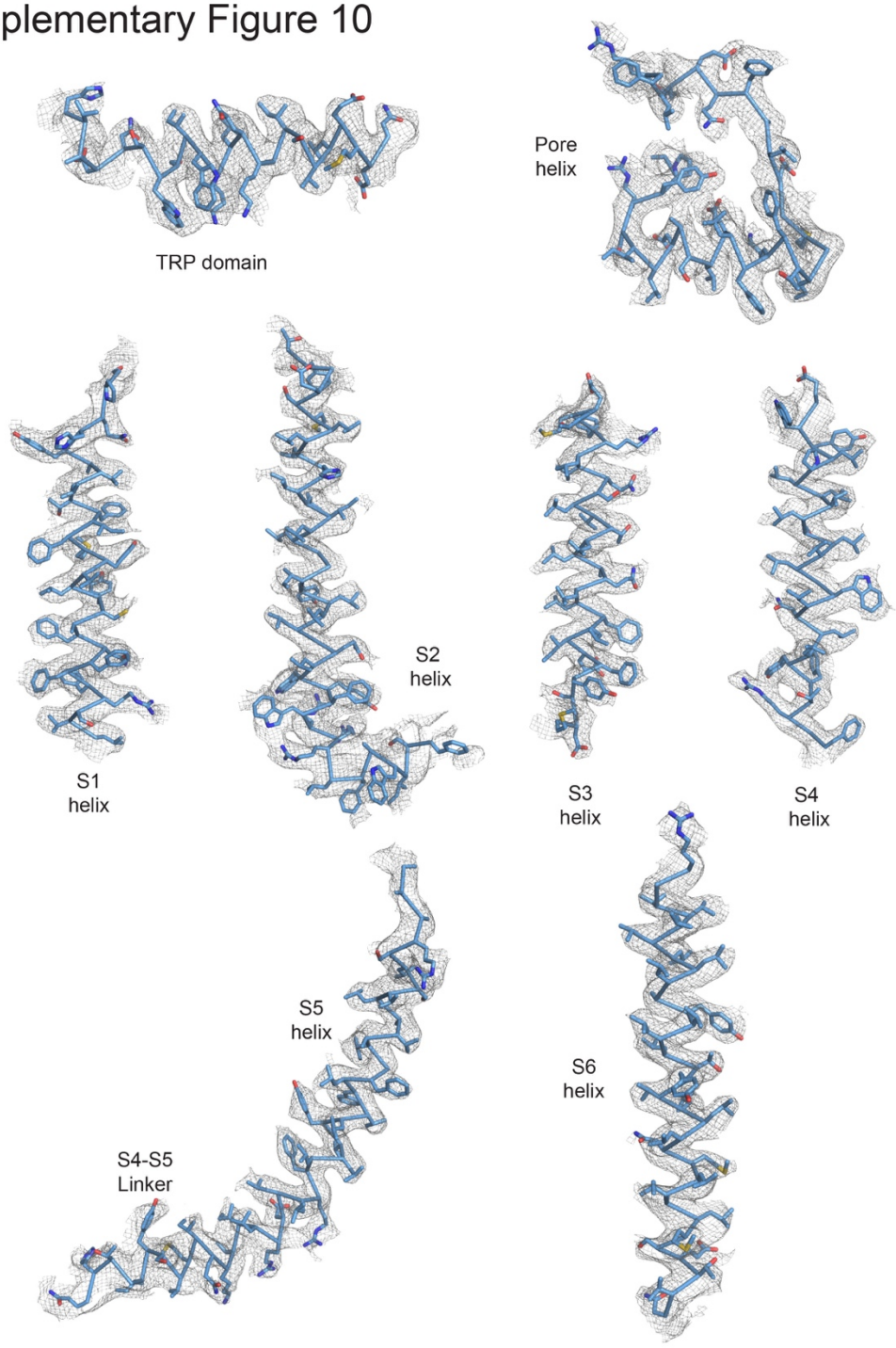

Supplementary Figure 10. Data quality of the CBD-bound TRPV2 in nanodiscs structure. Selected helices of the CBD-bound TRPV2 in the presence of PI(4,5)P_2 model (blue) overlaid with the corresponding cryo-EM density map in grey mesh. Side chains are shown as sticks and atoms are colored by element.

Supplementary Figure 11

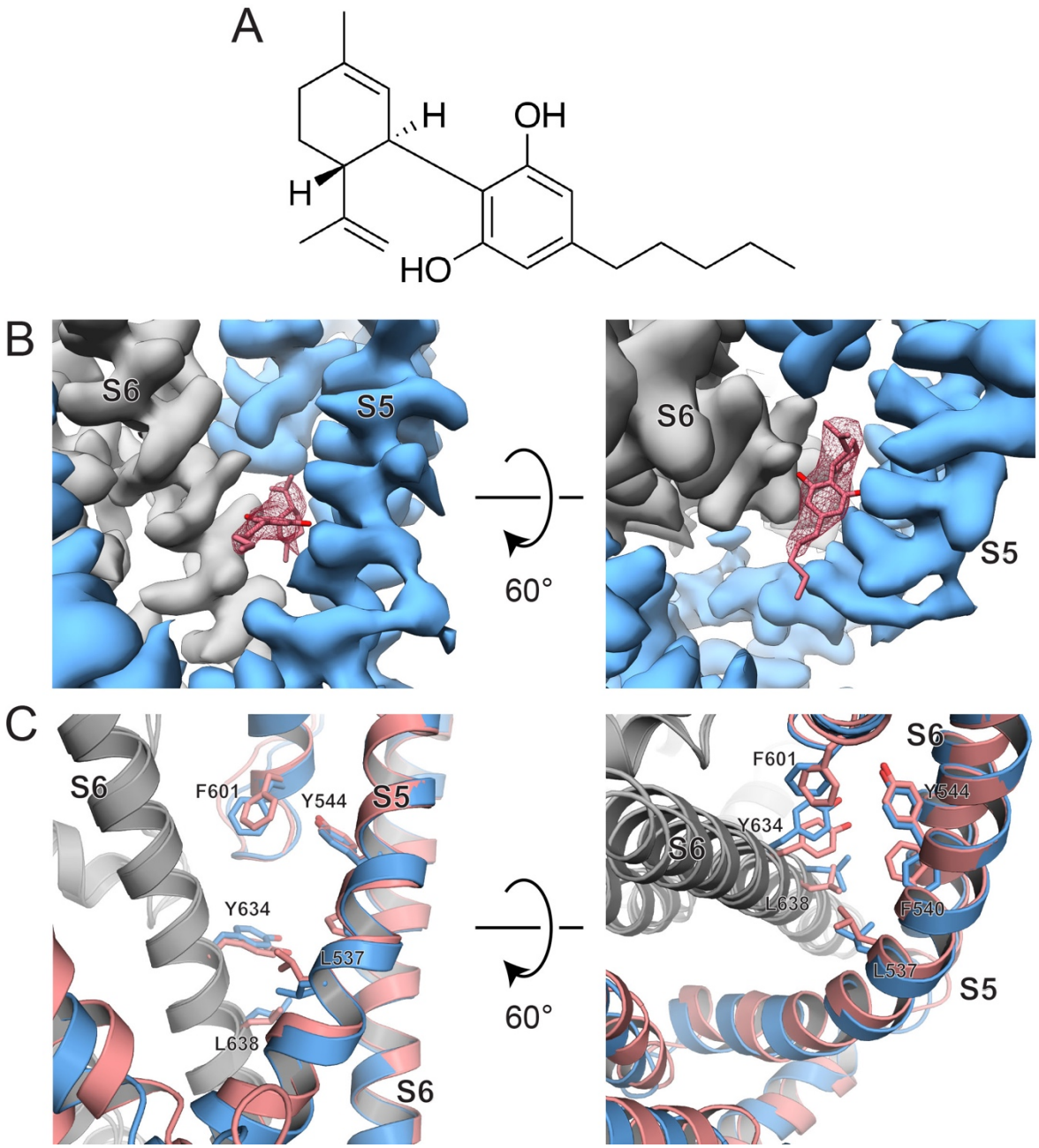

Supplementary Figure 11. CBD binding pocket. (**A**) Chemical diagram of molecular cannabidiol (CBD). (**B**) The CBD binding pocket of CBD-bound TRPV2 in PI(4,5)P_2 enriched nanodiscs. The electron density map of the S5 and S6 helices of TRPV2 are shown as blue and grey surfaces, respectively. The density attributed to bound CBD is shown as pink mesh and the chemical structure of CBD is shown as pink sticks. (**C**) Model representation of the CBD binding pocket. The model of the S5 and S6 helices of CBD-bound TRPV2 in nanodiscs are shown as blue and grey cartoons, respectively. This model is overlaid with the S5 and S6 helices of apo TRPV2 in detergent which are shown as pink and grey cartoons, respectively. Residues of interest are labeled and represented as sticks.

Supplementary Figure 12

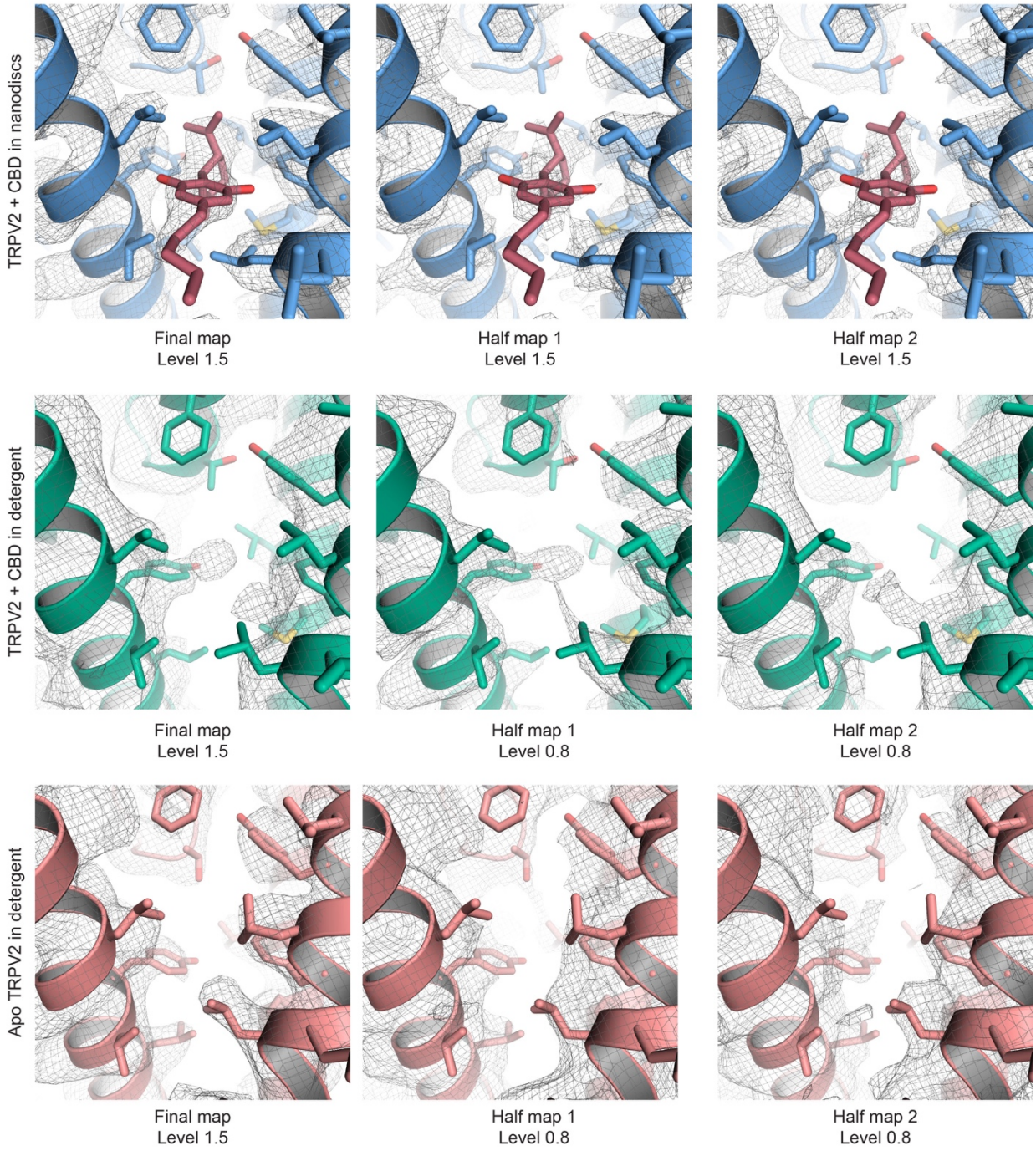

Supplementary Figure 12. CBD cryo-EM density. TRPV2 models overlaid with the sharpened density map and the two corresponding half maps for CBD-bound TRPV2 in PI(4,5)P_2 enriched nanodiscs (top, blue), CBD-bound TRPV2 in detergent (middle, green) and apo TRPV2 in detergent (bottom, salmon). Cryo-EM densities shown as grey mesh and side chains of interest are shown as sticks. Bound CBD (top) is shown as pink sticks.

Supplementary Figure 13

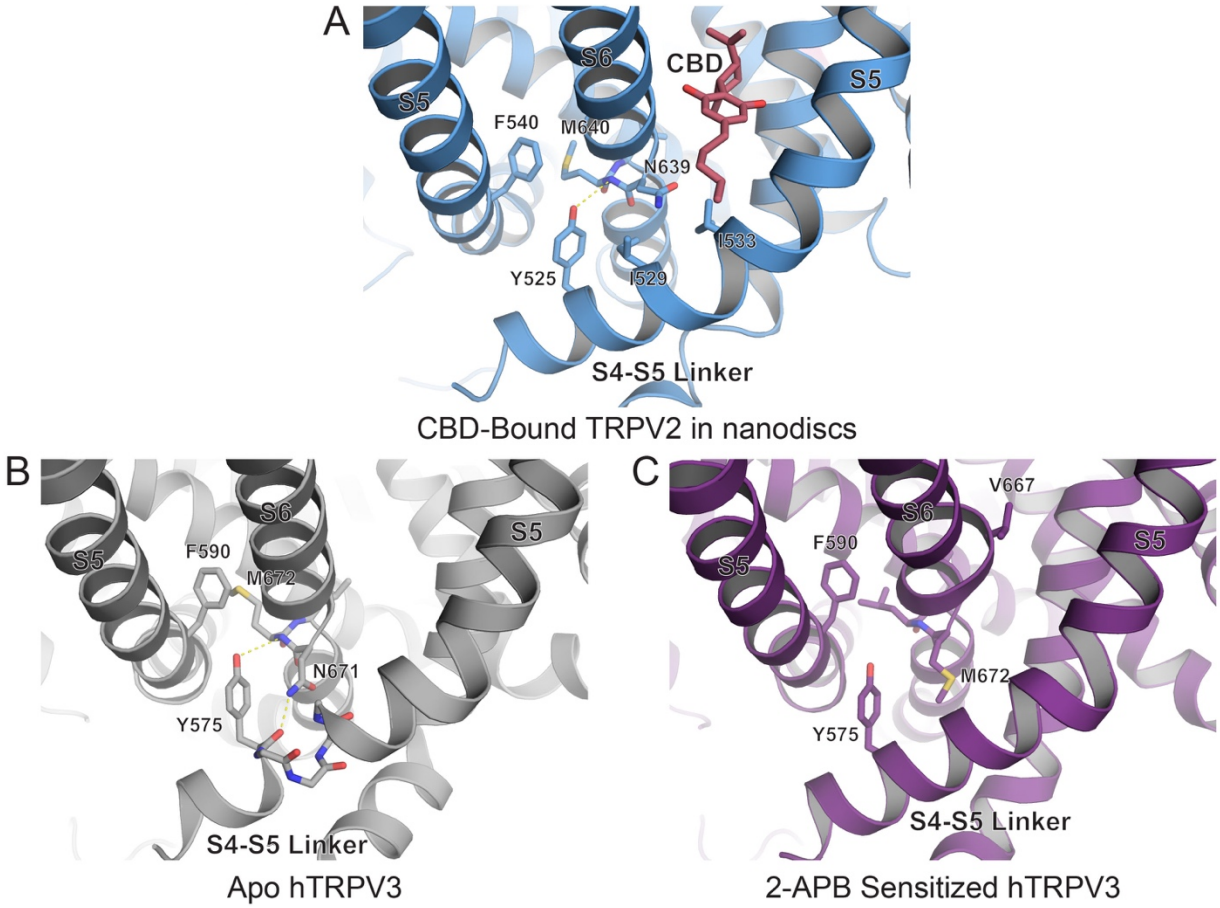

Supplementary Figure 13. (**A-C**) Area of helix breakage for (A) CBD-bound TRPV2 in nanodiscs, (B) apo human TRPV3 (PDB 6MHO) and (C) 2-APB sensitized human TRPV3 (PDB 6MHS). Residues of interest are labeled and shown as sticks.

Supplementary Figure 14

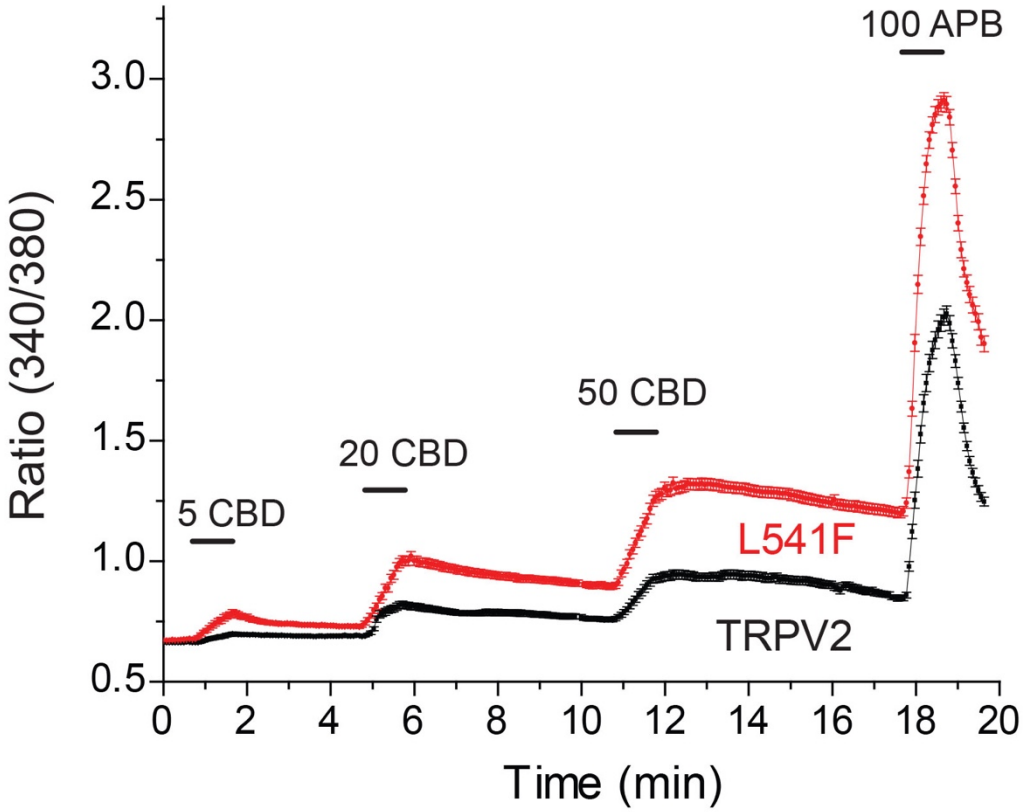

Supplementary Figure 14. The L541F mutation enhances CBD responses of TRPV2. Ca^{2+} imaging experiments on Fura-2 loaded HEK293 cells were performed as described in the methods section. The applications of 5 µM CBD, 20 µM CBD, 50 µM CBD and 100 µM 2-APB are indicated by the horizontal lines in cells transfected with wild-type rat TRPV2 (black) and the L541F mutant of TRPV2. The traces show mean +/- SEM from three different cover-slips, n=482 cells for wild type TRPV2 and n=613 for L541.

Supplementary Figure 15

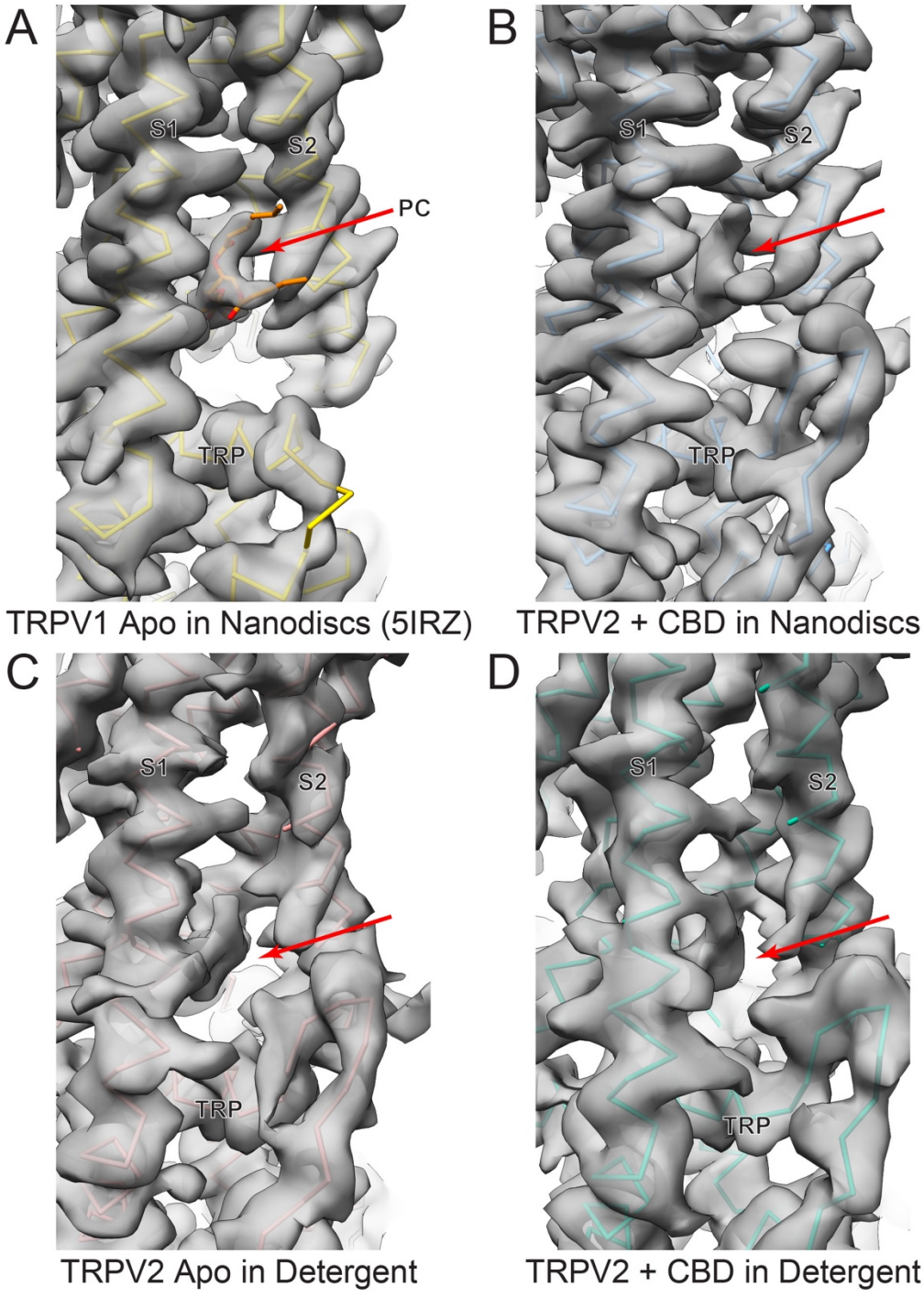

Supplementary Figure 15. Lipid binding pocket. The lipid binding pocket located between the S1, S2 and TRP helix of (**A**) apo TRPV1 in nanodiscs (PDB 5IRZ), (**B**) CBD-bound TRPV2 in $PI(4,5)P_2$ enriched nanodiscs, (**C**) apo TRPV2 in detergent, and (**D**) CBD-bound TRPV2 in detergent. The models for the helices that constitute the pockets are shown as ribbons and overlaid with their respective cryo-EM densities shown as grey surfaces. Arrows indicate the location of non-protein densities in these pockets.

Supplementary Figure 16

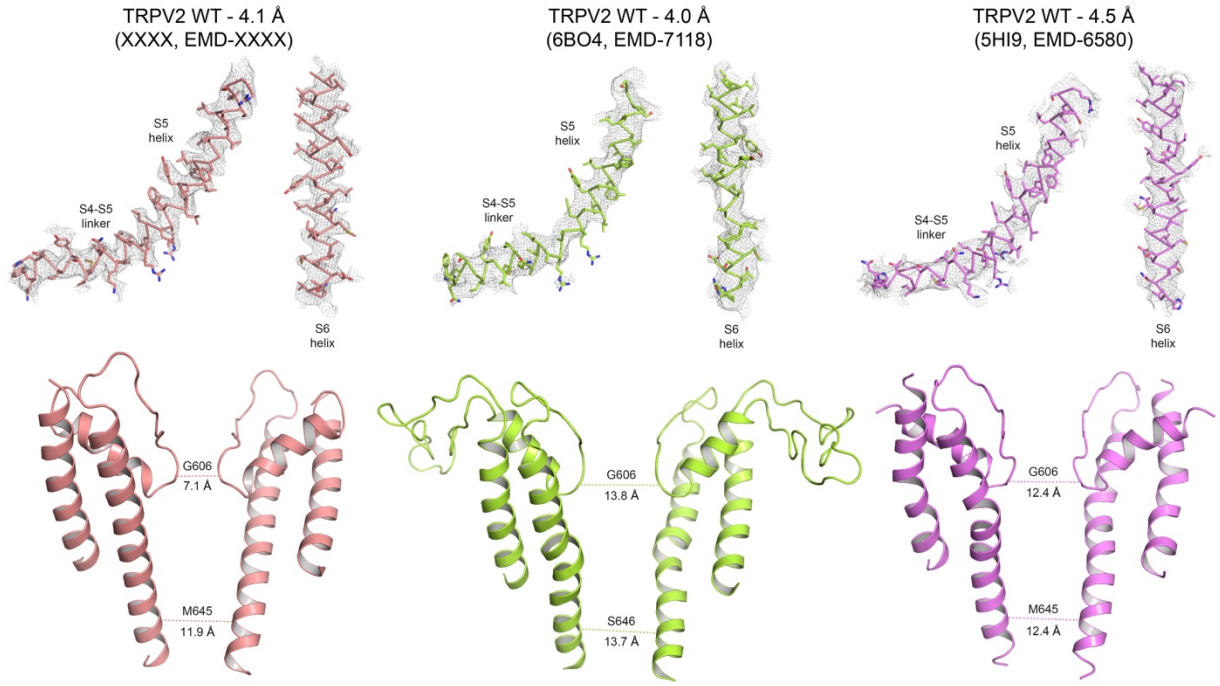

Supplementary Figure 16. Map quality and pore comparisons of WT TRPV2. Ribbon representation of the S4-S5 linker, S5 and S6 helices overlaid with their respective cryo-EM maps as well as the pore dimer cartoons for the reprocessed apo TRPV2 in detergent (salmon, left), TRPV2 in the open state (green, center) and the previously published apo TRPV2 (light pink, right). Cryo-EM maps are shown as grey mesh. Pore diameter measurements are from the carbon backbone of each model.

Supplementary Figure 17

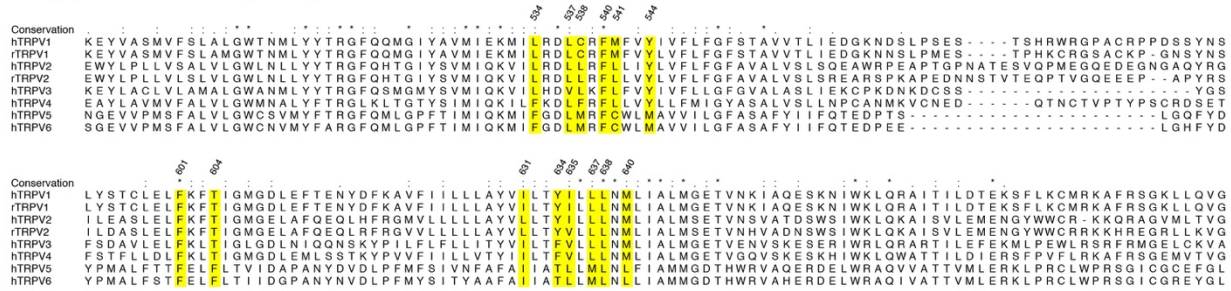

Supplementary Figure 17. Residue conservation in the CBD-binding pocket. Sequence alignment of select TRPV family channels of the S5-S6 region. Residues involved with CBD-binding are highlighted in yellow.

Supplementary Table 1. Cryo-EM data collection and model statistics

	CBD-bound TRPV2 in detergent (EMB-0462, PDB 6NNL)	CBD-Bound TRPV2 in Nanodiscs (EMB-0463, PDB 6NNM)	Apo TRPV2 in Detergent (EMB-0461, PDB 6NNK)
Data collection and processing			
Magnification	~18,000	~45,500	~31,000
Voltage (kV)	300	300	300
Defocus range (μm)	1.4-3.0	0.8-3.0	1.5-3.0
Pixel size (Å)	1.38	1.07	1.29
Symmetry imposed	C4	C4	C4
Initial particle images (no.)	820,953	685,702	420,081
Final particle images (no.)	49,496	43,608	33,941
Map resolution (Å)	4.3	3.8	4.1
FSC threshold	0.143	0.143	0.143
Map resolution range (Å)	3.5-5.5	3.0-5.0	3.5-5.5
Refinement			
Model resolution cut-off (Å)	4.3	3.8	4.1
FSC threshold	0.143	0.143	0.143
Map sharpening *B* factor (Å^2)	-200	-85	-139
Model composition			
Nonhydrogen atoms	0	0	0
Protein residues	2488	2464	2420
Ligands	0	4	0
R.m.s. deviations			
Bond lengths (Å)	0.006	0.007	0.007
Bond angles (°)	0.938	0.893	1.053
Validation			
MolProbity score	1.70	1.52	1.70
Clashscore	4.00	4.22	6.05
Poor rotamers (%)	0.50	0.37	0.56
Ramachandran plot			
Favored (%)	91.30	95.39	94.64
Allowed (%)	8.70	4.61	5.36
Disallowed (%)	0.00	0.00	0.00